UCRL- 99776
PREPRINT

A Detailed Kinetic and Thermodynamic Model of Petroleum Formation, Destruction, and Expulsion

Alan K. Burnham
Robert L. Braun

This paper was prepared for the
14th International Meeting on Organic Geochemistry
Paris, France, September 18-22, 1989

September, 1989

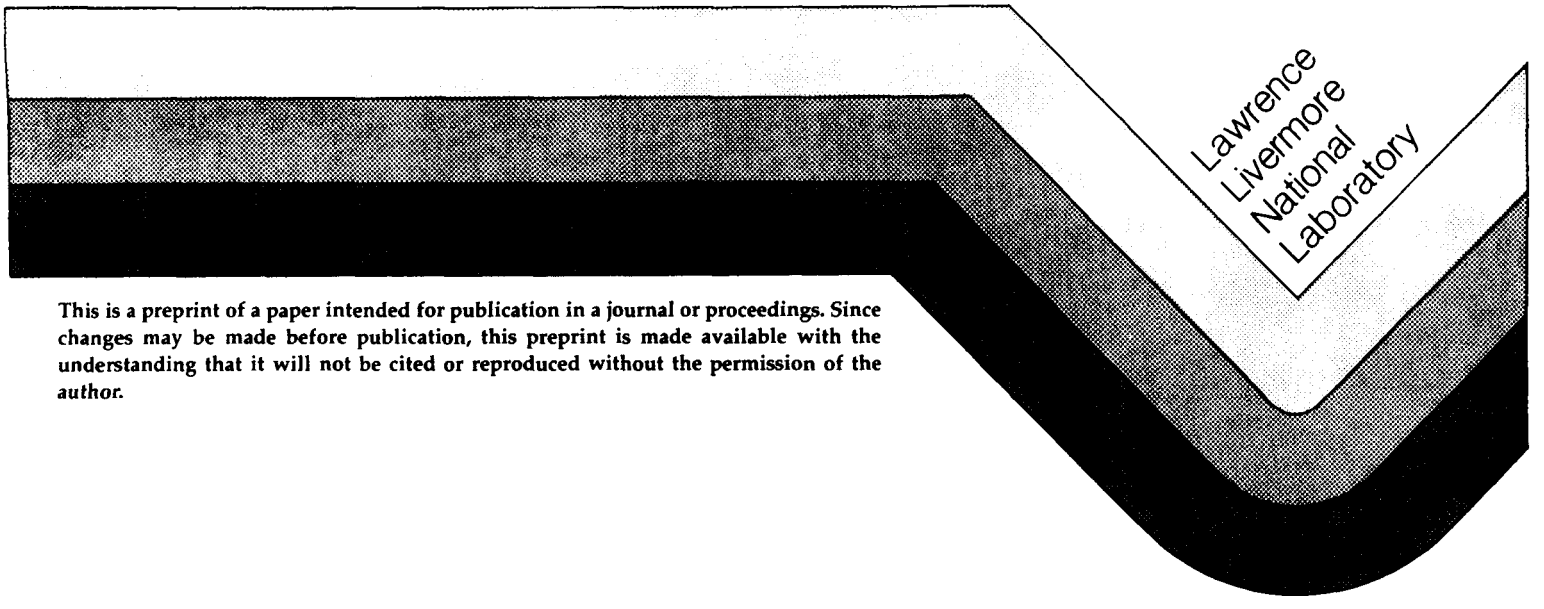

A Detailed Kinetic and Thermodynamic Model of Petroleum Formation, Destruction, and Expulsion

Alan K. Burnham and Robert L. Braun

Lawrence Livermore National Laboratory
P.O. Box 808, Livermore, CA 94550

UCRL--99776

DE90 000830

Running Head: Detailed model of petroleum formation

Key words: kerogen pyrolysis, petroleum generation, expulsion, migration, kinetics, phase equilibria, PVT calculations

Abstract—A variety of laboratory experiments, including programmed micropyrolysis, isothermal fluidized-bed pyrolysis, oil evolution from a self-purging reactor, pyrolysis-mass spectrometry, and hydrous pyrolysis are analyzed to derive chemical kinetic expressions for pyrolysis of lacustrine and marine kerogens. These kinetic parameters are incorporated into an improved, detailed chemical-kinetic model which includes oil and gas generation from kerogen, oil degradation by coking and cracking, gas generation from residual kerogen, and hydrogen consumption reactions. Oil is described by eleven boiling-point fractions. The model includes equation-of-state calculations of vapor/liquid equilibria and PVT behavior. The model can be run for closed, open, and leaky systems, and the open system can include an inert-gas purge. The porosity is calculated for both unconstrained conditions as well as a conditions simulating natural compaction and fracturing during sedimentary burial. Model calculations are compared to results from a variety of laboratory experiments, including hydrous pyrolysis. Oil expulsion efficiencies and properties are also calculated for a variety of geological conditions. The relative amounts of water and hydrocarbon phase(s) expelled are governed by saturation-dependent relative permeabilities. Gas/oil ratios in the expelled petroleum are related to organic content and geological heating rate.

INTRODUCTION

Although traditional petroleum exploration has emphasized locating traps by geophysical techniques, discovery efficiency can be increased if other factors such as source rock location, quality, quantity, maturity are considered (Demaison and Murris, 1984). Substantial progress has been made recently in developing quantitative models for conversion of kerogen to oil and gas (Lewan, 1985; Sweeney *et al.*, 1987; Tissot *et al.*, 1987; Mackenzie *et al.*, 1988). However, there is still a significant difference of opinion concerning the best experimental and mathematical methods for determining kinetic rate expressions. Moreover, the crucial consideration in most situations is the timing of petroleum expulsion from the source rock, not the timing of hydrocarbon generation. This means that it is important to understand the physical processes affecting transport out of the source rock.

A reoccurring tension when deriving kinetic models of oil and gas generation is the tradeoff between simplicity and completeness. Kerogen is a complex material that is

difficult to characterize in detail, and describing its thermal breakdown in detail is even more difficult. As a practical matter, all models must make use of "lumped" chemical species. Simple and complex models differ in how much lumping occurs. The definitions of the lumped species are usually tied to an experimental procedure. The measurement procedure may be tied to some chemical characteristics, but transport processes may also play an important role in the operational definition. For example, consider the lumped species *kerogen*, *bitumen*, *petroleum*, *oil* and *gas*. Kerogen and bitumen are defined as the portions of organic matter that are insoluble and soluble, respectively, in organic solvents. Unfortunately, extractability depends on solvent type, temperature, and even time because some "bitumen" molecules must diffuse out of the "kerogen" structure. An individual chemical may be partitioned between kerogen and bitumen. Hunt (1979) defines petroleum as a form of bitumen that can be produced through a drill pipe—a physical, not chemical, distinction. Petroleum consists of oil and gas, and the distinction is based on what condenses at standard temperature and pressure. Laboratory pyrolysis experiments have similar definitions. Oil (or tar in the case of coal) is usually defined as the pyrolysate that condenses in a trap external to the pyrolysis vessel. Gas is the uncondensed matter, and bitumen is the extractable matter left in the reactor. Again, these distinctions are based on volatility, which depends on temperature and pressure as well as chemical characteristics. If the reactor is operated at a different pressure, the volatility threshold for reaching the condenser changes. Therefore, when using one set of experiments to develop a chemical model of another situation, it is important to make sure that the physical processes contributing to the lumping procedure have been taken into account.

An additional impediment to modeling natural petroleum generation and maturation on the basis of laboratory experiments is that the time and temperature scales are very different. The Arrhenius equation, $\ln k = \ln A - E/RT$ in one form, is often used to describe the dependence of reaction time on temperature. It is an empirical equation, but detailed theoretical arguments give essentially the same functional form (Glasstone *et al.*, 1941). There are several potential pitfalls in extrapolating from laboratory to natural time-temperature regimes. First, one may have difficulty measuring the slope of ln k versus 1/T accurately enough to extrapolate adequately. This could be because of random errors such as detector noise or because of nonsystematic errors (*e.g.*, a temperature measurement error that is a function of temperature). Second, ln k may not be exactly linear in 1/T because of a change in the rate-limiting step or a change in the relative importance of competing mechanisms. This may occur for strictly chemical reasons or because of changing mass transport contributions if sufficient care has not been taken to remove them. Third, the rate law used may not be appropriate. Several authors (Anthony and Howard, 1976; Ungerer and Pelet, 1987; Burnham *et al.*, 1987, Quigley *et al.*, 1987; Solomon *et al.*, 1988; Burnham *et al.*, 1989) have used multiple parallel reactions having an activation energy distribution to mimic the complexity of kerogen pyrolysis. In addition, Braun and Burnham (1987) developed a fairly detailed picture of the errors introduced into the apparent E_a and A when activation energy distributions are ignored and when temperature and extent of conversion are not adequately decoupled.

One of the goals of our research is to develop a detailed model of oil and gas generation that can be used to probe the differences among various laboratory

experiments. If this model can account for the differences in product formation rates, amounts, and compositions over the very wide range of pyrolysis conditions accessed by different experiments, we can have more confidence in our ability to reliably predict transformations underground. The detailed model can also be used to determine which, if any, of the commonly used procedures lead to simple model parameters that are consistent with nature. Finally, the detailed model can be used to help derive improved simple models and improved experimental and mathematical procedures for deriving simple model parameters. To accomplish these tasks, the model must treat both chemical and physical (*e.g.*, transport) processes.

In this paper, we review the some of the results of our recent experiments in order to highlight the differences in Arrhenius parameters that can be derived from different experiments. We then use our detailed pyrolysis model, PYROL, to explain why these differences occur. The version of PYROL used here is a descendant of one developed in 1983 and described at several evolutionary stages (Burnham and Braun, 1985; Sweeney *et al.*, 1987; Braun and Burnham, 1989). Throughout its development, it has included equations that explicity describe both chemical reactions and product removal from the reactor by bulk flow. Although some changes have been made in the reaction network, the major recent improvement is in the PVT calculations. The original model used Raoult's law to calculate oil vapor partial pressures and the ideal gas law to calculate gas volume. The present version uses a corrected RKS equation of state to calculate phase equilibria and volumetrics (Péneloux *et al.*, 1982). All of our computer code development calculations used reaction parameters for Green River oil shale, a typical lacustrine deposit. In the process of comparing model calculations with experiments for this paper, we derived preliminary reaction parameters for generic marine oil shale. Backed by favorable comparisons between model calculations and various experiments, we make predictions for geological expulsion timing and efficiency over a wide range of conditions, assuming a compaction-aided bulk-flow mechanism. The effects of source rock permeabilibity and compaction are treated by a simple mechanical model. We also discuss crucial areas of uncertainty in the chemical mechanism and how they affect the reliability of oil and gas volumes calculated for geological conditions.

EXPERIMENTAL RESULTS

The four experimental techniques considered in most detail are shown in Figure 1. Except for hydrous pyrolysis (Lewan, 1985; Huizinga, 1988), the results presented here are mostly unpublished work from our laboratory. Only the parts of the procedures and results considered to be crucial to the major message of this paper will be presented here. Further details will be published elsewhere in a series of papers. Most of the samples used have been described elsewhere (Burnham *et al.*, 1987). LLNA is a La Luna sample (QL-7) provided by S. Talukdar of INTEVEP, and WNZN is a Toarcian shale (Lias ε, Wenzen core) provided by J. Rullkötter of KFA Jülich. Both WNZN and LLNA are high in carbonate.

Programmed Micropyrolysis. The potentially most useful method of measuring pyrolysis is by micropyrolysis. The apparatus most commonly used now by organic geochemists is one of the various Rock Eval models. A common problem in most Rock

Eval models is that the furnace profile is nonuniform (Espitalié, 1986; Burnham *et al.*, 1988a), and accurate temperature measurements are difficult. We attempted to circumvent this problem in the past by using "known" kinetics for a standard Green River shale sample (AP22) to calibrate the temperature (Burnham *et al.*, 1987). When analyzed by appropriate reaction models, this calibration procedure resulted in reasonable rate parameters, although a few of our published parameters seem to suffer from poorer precision than we originally thought. For example, a subsequent measurement on New Albany shale (Burnham *et al.*, 1988b) using the same procedure gave a mean E_a that was 5 kcal/mol higher than our earlier result (Burnham *et al.*, 1987).

More recently, we obtained a prototype model of Pyromat II (Lab Instruments, Inc.) for these measurements. We modified the furnace to improve temperature uniformity, achieving $\pm$1.5°C over the sample region at 400-500°C. We replaced the 1.6 mm diameter type K thermocouple (TC) with a 1.0 mm diameter grounded TC for better time response. We calibrated our thermocouples against one that had been standardized to a platinum RTD, and we calibrated the Pyromat electronics with several commercial temperature readouts. We estimate that our temperatures are accurate to $\pm$3°C absolute and $\pm$1°C relative. This does not ensure that the TC reflects the sample temperature, but the small sample size (15 mg whole rock or 1 mg kerogen), the good furnace uniformity, and the close proximity of the sample and TC suggest that the error is small. Volatilization rates were measured at heating rates ranging from 0.3 to 50°C/min, although only rates greater than 0.9°C/min were generally used in the kinetic analysis. The estimated standard deviation of T_{max} was about $\pm$1°C. Even with the finer TC, TC time constant measurements suggest that the measured temperatures at 50°C/min may be 1-2°C lower than the true value.

We have investigated numerous samples, nearly all of them as whole rocks. Our most extensive measurements are on sample AP22. We analyzed the data with the program KINETICS (version 2.1; Braun and Burnham, 1988) using an improved approximate (T_{max}-shift) method, modified Coates-Redfern and Friedman methods, and gaussian and discrete E_a distribution methods. Briefly, the measured T_{max} is within experimental precision of that calculated from $A = 1 \times 10^{13}$ s^{-1} and E_a = 51 kcal/mol for heating rates between 1 and 10°C/min. However, the measured T_{max} is a few °C lower at 50°C/min and a few °C higher at 0.3°C/min. Linear regression analysis of T_{max}-shift data gives $E_a = 53 \pm 1$ kcal/mol. The discrete model gave 7% of the reaction at 50 kcal/mol and 93% at 55 kcal/mol. The discrete model energies agree well with results presented by Ungerer *et al.* (1987), but we think that the activation energy from the T_{max} shift is more reliable for lacustrine kerogens for reasons discussed elsewhere (Burnham *et al.*, 1988b).

Rate parameters derived from Pyromat data using the gaussian E_a distribution model are given in Table 1 for AP22 and 6 other samples. A general observation is that the typical mean E_a for marine kerogens is about 53 kcal/mol rather than about 48 kcal/mol according to earlier measurements (Burnham *et al.*, 1987). Half of the difference is related to the use of 51 kcal/mol to calibrate the Rock Eval apparatus rather than the 53 kcal/mol measured by Pyromat. Another contribution may be related to the use of a lacustrine sample to calibrate temperatures for marine samples, as discussed earlier (Burnham *et al.*, 1988a).

Fluidized-Bed Pyrolysis. Coburn *et al.* (1988) have studied the pyrolysis of Green River and New Albany oil shales by dropping samples into a preheated, fluidized bed of sand. The pyrolysate is burned catalytically and the combustion products measured dynamically by mass spectrometry. They found that most of the long-time tail observed previously (e.g., Wallman *et al.*, 1981) is due to holdup in cool transfer lines. We determined new rate parameters for parallel 1st- and nth-order reactions by nonlinear regression using KINETICS. The thermal history included a realistic heatup time constant, and calculated rates were convoluted at each step with an experimental dispersion function before comparison to the measured rates. We previously showed (Burnham *et al.*, 1988b) that the deviations from first-order behavior are similar for constant-heating-rate and "isothermal" experiments. The principal activation energy reported in Table 1 for GRS sample AP24 is slightly different from that given earlier because of improved measurement of the dispersion function. The evolution rates from the fluidized bed are slightly faster than from Pyromat, corresponding to temperature differences of about 6°C for GRS and about 10°C for New Albany shale. This is qualitatively consistent with the concept of enhanced volatilization due to the extremely high gas sweep rates in the fluidized-bed experiment.

Oil Evolution. We have used oil evolution from a self-purging reactor, a descendant of a modified Fischer Assay apparatus, to measure kinetics for many years (Campbell *et al.*, 1978; Burnham and Singleton, 1983; Burnham *et al.*, 1988a). The type of kinetic data obtained is similar to the integral of that from Rock Eval and Pyromat, except that only oil is measured directly. One version (Burnham and Singleton, 1983) included a back-pressure regulator so that pyrolysis could occur at a pre-selected, elevated pressure. The present work used the same apparatus described by Burnham *et al.* (1988a), and much of the data analyzed here is reported in Figs. 3 and 4 of that paper. Temperature was measured with four 1 mm type-K TCs, each of which was calibrated against the same standardized type-K TC used to calibrate the Pyromat II thermocouples. The kinetic data were fitted to both the discrete and gaussian model using the measured time-temperature relationship (constant-heating-rate segment formalism, Braun and Burnham, 1987). Results for the gaussian model are shown in Table 1 for the five available samples. Note that an E_a distribution is needed for all samples. The σ value for GRS should not be taken too seriously because it is caused by the significant biomarker generation and bitumen volatilization prior to major oil generation.

Pyrolysis-Mass Spectrometry. We have reported rates of evolution of individual gas species from pyrolysis of lacustrine, marine, and terrigenous samples (Campbell *et al.*, 1980; Huss and Burnham, 1982; Coburn, 1983; Burnham *et al.*, 1987; Oh *et al.*, 1988; Burnham *et al.*, 1989; Reynolds *et al.*, 1989). Nearly all our experiments have used a pyrolysis furnace outside the mass spectrometer ionization chamber, a trap to condense heavy components, and a high ionization voltage to maximize signal intensity for fixed gases. Most experiments prior to 1986 used large (25-50g) samples of rock and a Dry Ice trap between the pyrolysis vessel and a single-quadrupole mass spectrometer. More recently, we have used a triple-quadrupole mass spectrometer (TQMS) for increased selectivity, increased the trap temperature to about 130°C to observe water and hydrocarbons up to about C_7, and decreased the required sample size to 0.5 g of rock for

experiments at 10°C/min and to 5 g for experiments at 1°C/min. Coal samples are mixed with quartz sand to behave like whole rock.

For oil exploration purposes, the pyrolysis-mass spectrometer experiments are designed to answer several related questions. First, are the kinetics of gas species the same as the oil? Are the E_a distributions necessary to characterize oil evolution by itself, as in Table 1, caused by different kinetics for different components, or do individual components need E_a distributions? Finally, can the sequence of gas evolution be used to understand the maturation mechanism? Although care was taken in the pyrolysis-TQMS experiments to account for most of the factors that could lead to erroneous temperature measurements, the complexity of the experiments and some problems with TC calibrations lead to uncertainties of 5-10°C in some experiments. For now, we are limited to qualitative and semi-quantitative conclusions about oil and gas kinetics. Even so, we can address the most important conceptual issues.

First, the kinetics of individual gas species are far more diverse than those for the total hydrocarbon generation. Acetic acid and CO_2 (after accounting for carbonate decomposition) tend to precede hydrocarbons and have very broad evolution profiles, suggesting large E_a distributions. Methane generation is also very broad, but it tends to lag oil generation. For Green River kerogen, methane has a large primary peak near that of oil generation and a higher temperature shoulder probably related to elimination of residual methyl groups and methylene bridges in the highly aromatic residue remaining after oil generation. For marine and terrigenous samples, the first peak is smaller than the second. Hydrogen shows similar features. H_2S, COS, mercaptans, and, to a lesser extent, methyl thiophene tend to evolve at lower temperatures than hydrocarbons. For molecules containing 4-7 carbons, aliphatic profiles tend to be narrower than aromatic profiles. Since the shift with heating rate is about the same, the aromatic materials require wider E_a distributions. Unfortunately, the absolute value of the distribution is compromised by tailing of these oil components through the trapping system. Qualitatively, the pyrolysis-TQMS results confirm for many samples that oil generation by itself needs an E_a distribution for proper kinetic description and that, although the gas evolution processes are more diverse than oil generation processes, the distributions determined for total hydrocarbons by micropyrolysis are not caused solely by inclusion of gas. This agrees with the results of Espitalié *et al.* (1988).

PYROL

Model description. A detailed description of the current version of PYROL is given elsewhere (Braun and Burnham, 1989), so only a limited description will be given here. The chemical reaction framework of PYROL is given in Figure 2. Oil consists of eleven boiling point fractions, each having two chemical types, cokable and uncokable. The rate constants used for Green River shale (GRS) are also given by Braun and Burnham (1989), and only changes from a previous version (Sweeney *et al.*, 1987) will be highlighted here. The rate expressions for oil generation have been changed slightly to be consistent with our assumed standard kinetics (Burnham *et al.*, 1987). The activation energies of oil coking and cracking have been increased to 45 and 55 kcal/mol, respectively, with corresponding adjustments to the frequency factors. The cracking rates for cokable oil have been set to zero, and oil coking frequency factors now depend on

molecular weight in the same way that cracking does. The pressure dependence of oil cracking has been decreased, and rate constants have been included for cracking of C_2-C_4 gas to methane and coke.

We have also derived preliminary reaction parameters for marine oil shales. They differ from those for GRS in the following ways. The initial bitumen content is decreased from 5 to 2 wt%. Oil generation is described by a single process having a mean E_a the same as for the principal oil generation from GRS (51 kcal/mol), but a gaussian σ of 3% is used and the frequency factor is 2.4 times faster. Gas generation rate constants were estimated from pyrolysis-TQMS experiments. The oil cracking rate parameters are the same as for GRS. The maximum possible oil and gas yields were estimated from the fluidized-bed pyrolysis results for New Albany shale (Coburn *et al.*, 1988). The H/C ratios of cokable and uncokable oil were assumed to be the same as for GRS, and the fraction of cokable oil was estimated from H/C ratios of pyrolysates. The initial cokable fraction of 0.68 is substantially higher than the 0.25 value for GRS, which is a reflection of the higher aromatic content of the initial kerogen and pyrolysates (Netzel and Miknis, 1982; Horsfield, 1989). The base frequency factor for oil coking was adjusted to give the correct oil yield for Fischer assay pyrolysis. The resulting lower oil yields at slower heating rates are consistent with the results of Coburn and Rubel (1983).

Bitumen, though defined operationally and not chemically, is an important quantity. Our original hope was that bitumen would be calculated directly from the amount of liquid oil. We explored the possibility of having the molecular weight of the largest component comparable to the maximum size found by FIMS measurements of heated-grid pyrolysates (Suuberg *et al.*, 1987), but we could not find a satisfactory set of parameters that maintained correct oil and gas yields for other pyrolysis conditions. Instead, we added a virtual bitumen component in a way that minimized changes in other parts of the code. A specified fraction of kerogen converts to virtual bitumen (and no other products) by a single first-order reaction. Virtual bitumen subsequently breaks down to oil, gas, and semicoke identically to kerogen, so it might also be considered to be soluble kerogen or asphaltenes. This reaction formalism is consistent with a highly branched kerogen structure that has large, potentially soluble blocks that are connected by weak links (Burnham *et al.*, 1988b). The additional parameters are the fraction of oil that goes through a bitumen and the rate constant. For GRS, the rate constant was based on work by Robinson and Cummins (1960) and the fraction was fixed at 0.25 to match hydrous pyrolysis experiments. For generic marine oil shale, the fraction was increased to 1.00 and the rate constant decreased to match hydrous pyrolysis results (Lewan, 1985).

The new phase equilibria and volumetric calculations in PYROL are also described in detail by Braun and Burnham (1989). Briefly, the phase equilibria are calculated using the Redlich-Kwong-Soave equation of state (Soave, 1972). The traditional flash calculational approach was found to be not very compatible with the differential equation solver used to integrate the chemical reactions. We therefore adopted a kinetic approach to phase equilibria similar to our earlier simple vaporization treatment. Basically, the rate of transfer between phases is multiplied by a function of relative fugacities that goes to zero at equilibrium. The rate constants for phase-transfer are adjusted to ensure a close approach to equilibrium without consuming too much computer time. The phase volume calculations were made more accurate by applying volume translation corrections

(Péneloux *et al.*, 1982). To check the accuracy of the equation of state calculations, methane solubility in oil was calculated at several relevant temperatures and pressures. Calculated solubilities agree very well with measured values (Price, 1984).

Laboratory Pyrolysis Applications. An extensive comparison of calculated oil and gas yields with various laboratory experimental results for Green River oil shale is presented elsewhere (Burnham and Braun, 1989). Agreement is very good and comparable to a previous version (Burnham and Braun, 1985). In this section we present comparisons for generic marine oil shale, some additional calculations for both Green River and marine shales that will help explain differences among rate parameters determined from various laboratory experiments, and a discussion of the oil expulsion mechanism in hydrous pyrolysis.

We demonstrate the ability of PYROL to calculate product distributions for both lacustrine and marine rocks for conditions used in many kinetics experiments. Calculated and observed distributions of organic carbon in oil, gas, and residue are given in Table 2. The product yields from marine shale are a function of pyrolysis conditions in ways similar to Green River shale. However, because of the higher fraction of cokable oil in marine kerogen pyrolysates, the marine kerogen yields are a stronger function of heating rate when expressed in terms of a percentage of Fischer assay yield. The sum of oil and hydrocarbon gas (CO_X excluded) is 580 mg/g TOC for the fluidized bed and 469 mg/g TOC for Fischer assay. For comparison, Rock Eval analysis gave S2 = 595 mg/g TOC for our New Albany sample. Calculated oil evolution curves are compared to measurements in Figure 3, and agreement is good. The difference between the 50% completion points of the calculated oil generation and evolution curves at 2°C/h is about 5°C, which is comparable to the remaining discrepancy between the calculated evolution curve and measurement.

We next attempt to explain the results in Table 1. The activation energies determined by oil evolution from the self-purging reactor are systematically higher than those determined by Pyromat, and the Pyromat activation energies are higher than those determined by fluidized bed. Our explanation is essentially the same as that given earlier (Burnham *et al.*, 1988a), although we now have more complete evidence. All these experiments measure the rate of volatilization, not generation. The rate of volatilization is affected by the amount of gas sweep. Volatilization is affected less at high temperatures because the pyrolysis products are more volatile. This causes the apparent activation energy to be inversely related to the amount of gas sweep.

This explanation is quantified in Table 3. PYROL was used to generate synthetic reaction rate data for conditions comparable to those in the experiments in question. The oil generation calculations used a mean activation energy of 51 kcal/mol for both lacustrine and marine shales. The resulting volatilization rates are a function of both the chemical and physical processes in PYROL. The output rates from PYROL were then fitted as real experimental data with the program KINETICS. The observed trends in activation energy are similar to those seen experimentally. The change in absolute volatilization rate is small compared to the shift in the activation energy, so the frequency factors also change to compensate.

Hydrous pyrolysis is more like nature than most other experimental techniques, and Lewan (1985) has derived kinetics describing the formation of a free-floating oil

phase during hydrous pyrolysis. However, as we mentioned in a previous paper (Burnham *et al.*, 1988a), it is not obvious that the reported rate constants are free of mass transport contributions. We now use PYROL to assess the role of mass transport in hydrous pyrolysis. Hydrous pyrolysis is difficult to model with PYROL because it consists of an open system (rock chip) inside a closed system. First, we calculate the product distribution in the whole closed system. We then assume, for simplicity, that all oil in the vapor state just prior to cool down will be expelled from the rock chips. These calculations for Green River and marine shales are shown in Figures 4 and 5 along with published data. The calculated bitumen curve is a combination of liquid oil, virtual bitumen, and semicoke. The calculated oil-vapor curves agree qualitatively with the expelled-oil data except in the 330°C region for Green River shale. A seemingly plausible explanation is that some liquid oil would be forced out by the oil vapors in that region. However, even though our initial assumption that all vapor will be expelled sounds reasonable, the oil vapor volumes at the high pressures generated inside the vessel are actually not large enough to expel much oil by bulk flow. We discovered this by using the calculated pressures from the first calculation (ranging from 9 to 48 MPa) as input to a second set of calculations, represented by the dashed line, in which the rock chips were treated as an open system with a time-dependent external pressure. While expulsion due to excess volume generation may be important during the first part of oil generation, it is inadequate in the latter stages. We therefore conclude that, without shale compaction, excess volume generation is inadequate to expel major quantities of oil. We suspect that the correlation of observed results with calculated volatility is symptomatic of the importance of another temperature- and composition-dependent mechanism, *e.g.*, diffusion.

We can also use the PYROL calculations to test the importance of various factors influencing the single-first-order rate parameters derived by Lewan (1985) and Peters (1986; obtained by analysis of the hydrous pyrolysis data in Huizinga *et al.*, 1988). We noted earlier (Burnham *et al.*, 1988a) that Lewan's activation energies are higher than expected if one considers only his neglect of activation energy distributions. Ordinarily, analyzing a complex reaction with a first order rate law, when temperature and conversion are not decoupled, will give an apparent activation energy that is smaller than the true mean value (Braun and Burnham, 1987). We proposed (Burnham *et al.*, 1988a) that the temperature dependence of the expulsion mechanism introduces a compensating error, thereby producing about the correct answer. Assuming that the good agreement between PYROL calculations and widely varied experimental observations means that PYROL is a good description of reality, we can use a kinetic analysis of the PYROL results as a test, at least in qualitative terms, of this proposal. The oil vapor yields were fitted by linear regression to a first order rate expression just as Lewan (1985) and Peters (1986) analyzed expelled-oil data, and the results are given in Table 3.

The apparent activation energy of 63.7 kcal/mol for Green River is much higher than the input value of 51 kcal/mol because only the volatility effect is present. Likewise, Peters' experimental value of 66.5 is higher than the "true" value of 50-52 kcal/mol (Sweeney *et al.*, 1987, Burnham *et al.*, 1987, Freund and Kelemen, 1989) because Green River shale has a small activation energy distribution and the volatility effect dominates. For marine shale, the apparent activation energy of 42 kcal/mol is

lower than the input mean value of 51 kcal/mol, but it is higher than the 33 kcal/mol value expected from the neglect of the activation energy distribution only. Our 42 kcal/mol value is in the same range observed by Lewan for Phosphoria shale. These results suggests that, when data that do not decouple temperature and conversion are analyzed by first-order rate equations, the apparent activation energy can be either higher or lower than the true mean value, depending on whether the activation energy distribution or volatility effects dominate. For both of the first-order analyses of the simulated hydrous pyrolysis data, the correlation coefficients were high (0.991 for marine and 0.975 for Green River). Therefore, a high correlation coefficient does not ensure a correct answer. In the case of the very low activation energies reported by Barth *et al.* (1989) for CO_2, acetic acid, and methane, preliminary kinetics determined from our pyrolysis-TQMS experiments indicate that the neglect of activation energy distributions is dominant in their case.

Geological Applications. PYROL includes a simple compaction model, expressed as a differential equation, that can be integrated simultaneously with the other differential equations. The compaction model is shown schematically in Figure 6. We normally treat sediments as leaky reactors, where the rate of product elimination is proportional to the pressure difference between the pore pressure and hydrostatic pressure. The product volume, porosity, and pore pressure are interdependent. In the absence of any better method, we use the relative permeability values of Ungerer *et al.* (1984) to calculate the relative volumes of water and hydrocarbon expelled. Gas and oil, if present as distinct phases, are expelled in proportion to their volume fractions. Diffusion and solubility of oil and gas in water are neglected, as currently is the thermal expansion of water.

We have conducted a few parameter studies for both lacustrine and marine source rocks. The results for lacustrine source rocks are described in more detail elsewhere (Braun and Burnham, 1989), and only a summary is given here. We present a few similar results for marine shales in Figures 7 to 10. For both lacustrine and marine rocks, sufficient overpressure was developed during oil and gas generation to noticeably hinder compaction of the source rock over all parameter ranges studied. The pore pressure exceeded lithostatic pressure only for the richest lacustrine shale at the highest heating rate. Oil expulsion is significantly delayed from oil generation. The amount of delay is inversely related to initial total organic content (TOC). During the delay, part of the oil is cracked to gas, which provides part of the volume generation needed for oil expulsion. As a result, the amount of oil cracking is also inversely related to organic content. The start of significant oil expulsion is subjective, but the concentration of oil at the start of expulsion varies ranges from about 14 mg oil/g rock for 10 wt% initial lacustrine TOC to 1.4 mg oil/g rock for 1 wt% initial marine TOC. However, the latter expellate is really a condensate, and a more reasonable minimum value (for 3 wt% marine TOC and 1 wt% lacustine TOC) is about 4 mg oil/g rock. Other product parameters for lacustrine and marine shales are compared in Table 4. Expulsion efficiencies were strongly affected by organic content but not by heating rate. The expelled gas/oil ratios and API gravity of the oil are inversely related to organic content. The amount of unexpelled gas at 200°C is roughly independent of original organic content. For the leanest rocks, even though most of the oil was cracked to gas, the excess volume generation was insufficient to expel most of the gas. All these results

depend on the equilibrium porosity-depth relationship, of course, but we have not yet investigated that dependence.

These geological results have been presented without comparison to field results. We intend to do extensive comparisons in the future, but a few initial comparisons are given here. The maximum C_{15+} concentrations of 100-300 mg/g lacustrine TOC is similar to that reported by Tissot *et al.* (1978). The corresponding range of 50-72 mg/g marine TOC is on the low side but similar to that reported by Larter (1988) for North Sea Viking Graben Kimmeridge clay samples. Our thresholds for significant oil expulsion are significantly higher than the 0.8 mg/g (15 bbl/acre-ft) minimum given by Momper (1978). His low value is inconsistent with our assumptions of a 5-10% porosity during generation and a relative permeability that requires about 30% oil saturation before much oil is expelled. However, our results agree with Talukdar *et al.* (1987), who state that the beginning of oil migration in the La Luna formation is at 200 mg bitumen/g TOC, which corresponds to 10 mg/g rock for 5% TOC (about average for that formation).

A serious issue is whether PYROL is accurately calculating the maximum possible geological oil yield. Our reaction parameters require that all cokable oil is converted to gas and coke fairly easily in the geological environment. This means that the maximum oil yield for geological conditions is 674 mg/g for lacustrine kerogen and 169 mg/g for marine kerogen. These are substantially lower than typical Rock Eval hydrogen indices, especially for the marine shale. The corresponding "primary" gas yields are also higher than generally assumed. We agree with Cooles *et al.* (1986) that oil expulsion efficiency can be a very efficient process, but we think that much of their observed efficiency for marine may be due to gas expulsion, both natural and that occurring during sample retrieval. Our reaction network is also in conflict with the proposal by Cooles *et al.* (1986) that laboratory pyrolysis produces the same amount of or more coke than geological maturation. The conversion of kerogen to oil, gas and coke can be considered to be a disproportionation reaction. For a specified H/C ratio in kerogen, oil and coke, the ratio of oil to coke depends on the fraction of hydrogen consumed by making gas (and water). If the geological mechanism really produces less gas than predicted by PYROL, then more oil would be possible. Our calculated oil yields agree well with both hydrous pyrolysis and the 1°C/week sealed-vessel experiments of Saxby (1986), so the evidence seems to support us for lacustrine kerogen. Although our treatment of hydrous pyrolysis is consistent with the amount of expelled oil, we underestimate the amount of bitumen for Woodford shale in the later stages. This could indicate that our oil coking reaction (and perhaps oil cracking reaction) should be inhibited by water, but there is not enough evidence available to determine the necessary rate parameter. The maximum oil potential is such an important question that further evidence is desirable.

A possibly important observation in this regard is that the yield of normal alkanes plus alkenes from our self-purging reactor is only about 2% of the kerogen TOC for both Kimmeridge and Phosphoria shales (Burnham, 1989). The total amount of normal moieties of reasonable length (determined by ^{13}C NMR) is only about 5% of the kerogen TOC. Corresponding values for Green River shale are 9.6% and 22%, respectively. We also know that the isoprenoid/normal ratios from these experiments are similar to those in natural petroleum (Burnham and Singleton, 1983). Therefore, if normal alkanes are to make up a major portion of crude oil, say 25%, and secondary generation of long-chain isoprenoids is not easy, natural crude oil yields must be significantly lower than those

produced by rapid pyrolysis. Therefore, geological pyrolysis must be producing more coke and more gas than typical laboratory pyrolysis.

CONCLUSIONS

Laboratory experiments can be used, when properly analyzed, to develop a fairly complete kinetic picture of kerogen pyrolysis. We have summarized our understanding into a detailed kinetic model called PYROL. Both lacustrine and marine kerogens pyrolyze to oil, gas, and coke with a mean activation energy of about 51 kcal/mol. The frequency factor for marine kerogen is greater, possibly related to a more branched kerogen structure, and an activation energy distribution is required. Mass transport contributes to the observed volatilization rate in many experiments and can lead to an apparent activation energy that is higher than the true value. Also, there does not seem to be enough excess volume generated for bulk flow to be an effective mechanism of oil expulsion during normal (no lithostatic load) hydrous pyrolysis experiments.

Extrapolation of our understanding of oil and gas generation to geological conditions by using PYROL gives some interesting results. Bulk flow does appear to be a fairly effective means to expel petroleum from rich source rocks. For lean source rocks, a large amount of oil cracking is required to generate sufficient excess volume, so lean lacustrine and marine source rocks are a better source of gas than oil. For very lean rocks, most of the generated gas remains in the rock as long as the porosity is several percent. Our calculated oil/gas ratios depend crucially on whether more or less coke and gas is formed geologically than in the laboratory.

Acknowledgements— This work performed under the auspices of the U.S. Department of Energy by the Lawrence Livermore National Laboratory under Contract W-7405-Eng-48. It was supported by the USDOE Offices of Basic Energy Sciences and Fossil Energy and a group of eight industrial sponsors (Arco, Exxon, Chevron, JNOC, Norsk Hydro, IKU, Statoil and Saga). We appreciate the experimental contributions of G. Frohwein, G. Koskinas, J. Clarkson, R. Simons, J. Reynolds, R. Crawford, R. Ward, T. Coburn, and R. Taylor.

REFERENCES

Anthony D. B. and Howard J. B. (1976) Coal devolatilization and hydrogasification. *AIChE Journal* **22**, 625-656.

Barth T., Borgund A. E. and Hopland A. L. (1989) Generation of organic compounds by hydrous pyrolysis of Kimmeridge oil shale—bulk results and activation energy calculations. *Org. Geochem.* **14**, 69-76.

Braun R. L. and Burnham A. K. (1987) Analysis of chemical reaction kinetics using a distribution of activation energies and simpler models. *Energy & Fuels* **1**, 153-161.

Braun R. L. and Burnham A. K. (1988) KINETICS: a computer program to analyze chemical reaction data. Lawrence Livermore National Laboratory Report UCID-21588.

Braun R. L. and Burnham A. K. (1989) A mathematical model of oil generation, degradation, and expulsion. submitted to *Energy & Fuels.*

Burnham A. K. and Singleton M. F. (1983) High pressure pyrolysis of Green River oil shale. In *Geochemistry and Chemistry of Oil Shales, ACS Symposium Series* **230** (Edited by F. Miknis and J. McKay) pp. 335-351. American Chemical Society, Washington, D.C.

Burnham A. K. and Braun R. L. (1985) A general kinetic model of oil shale pyrolysis. *In Situ* **9**, 1-23.

Burnham A. K., Braun R. L., Gregg, H. R. and Samoun A. M. (1987) Comparison of methods for measuring kerogen pyrolysis rates and fitting kinetic parameters. *Energy & Fuels* **1**, 452-458.

Burnham A. K., Braun R. L., and Samoun A. M. (1988a) Further comparison of methods for measuring kerogen pyrolysis rates and fitting kinetic parameters. In *Advances in Organic Geochemistry 1987, Org. Geochem.* **13**, 839-845.

Burnham A. K., Braun R. L., Taylor R. W. and Coburn T. T. (1988b) Comparison of isothermal and nonisothermal pyrolysis data with various rate mechanism: implications for kerogen structure. *Prepr. ACS Div. Petr. Chem.* **34**(1), 36-34.

Burnham A. K., Oh M. S., Crawford R. W. and Samoun A. M. (1989) Pyrolysis of Argonne premium coals: activation energy distributions and related chemistry. *Energy & Fuels* **3**, 42-55.

Burnham A. K. (1989) On the validity of the pristane formation index. *Geochim. Cosmochim. Acta* **53**, 1693-1697.

Campbell J. H., Koskinas G. J. and Stout N. D. (1978) Kinetic of oil generation from Colorado oil shale. *Fuel* **57**, 372-376.

Campbell J. H., Koskinas G. J., Gallegos G. and Gregg M. (1980) Gas evolution during oil shale pyrolysis. 1. nonisothermal rate measurements. *Fuel* **59**, 718-726.

Coburn T. T. (1983) Eastern oil shale retorting: gas evolution during pyrolysis of Northeastern Kentucky shales. *Energy Sources* **7**, 121-150.

Coburn T. T. and Rubel A. M. (1983) Comments on the modified Fischer assay of eastern oil shales of Kentucky. *Fuel Processing Technology* **8**, 1-12.

Coburn T. T., Taylor R. W., Morris C. J. and Duval, V. (1988) Isothermal pyrolysis and char combustion of oil shales. In *Proc. International Conf. on Oil Shale and Shale Oil* (Edited by Z. Yajie), pp. 245-252. Chemical Industry Press, Beijing.

Cooles G. P., Mackenzie A. S. and Quigley T. M. (1986) Calculation of petroleum masses generated and expelled from source rocks. *Advances in Organic Geochemistry 1985, Org. Geochem.* **10**, 235-245.

Demaison G. and Murris R. J. (1984) *Petroleum Geochemistry and Basin Evaluation, AAPG Memoir 25*, AAGP, Tulsa.

Espitalié J. (1986) Use of Tmax as a maturation index for different types of organic matter. Comparison with vitrinite reflectance. In *Thermal Modeling in Sedimentary Basins* (Edited by J. Burris), pp. 475-496. Technip, Paris.

Espitalié J. (1988) Primary cracking of kerogens. Experimenting and modeling C_1, C_2-C_5, C_6-C_{15}, and C_{15+} classes of hydrocarbons formed. In *Advances in Organic Geochemistry 1987, Org. Geochem.* **13**, 893-899.

Freund H. and Kelemen S. R. (1989) Low-temperature pyrolysis of Green River kerogen. *AAPG Bulletin* **73**, 1011-1017.

Glasstone S., Laidler K. J. and Eyring H. (1941) *The Theory of Rate Processes*, pp. 25-27, 191-193. McGraw-Hill, New York.

Huizinga B. J., Aizenshtat Z. A. and Peters K. E. (1988) Programmed pyrolysis-gas chromatography of artificially matured Green River kerogen. *Energy & Fuels* **2**, 74-81.

Horsfield B. (1989) Practical criteria for classifying kerogens: some observations from pyrolysis-gas chromatography. *Geochim. Cosmochim. Acta* **53**, 891-901.

Hunt J. M. (1979) *Petroleum Geochemistry and Geology*, pp. 28. Freeman, San Francisco.

Larter S. (1988) Some pragmatic perspectives in source rock geochemistry. *Marine and Peroleum Geology* **5**, 193-204.

Lewan M. D. (1985) Evaluation of petroleum generation by hydrous pyrolysis experimentation. *Phil. Trans R. Soc. Lond. A* **315**, 123-134.

Mackenzie A. S. and Quigley T. M. (1988) Principles of geochemical appraisal. *AAPG Bulletin* **72**, 399-415.

Momper J. A. (1978) Oil migration limitations suggested by geological and geochemical considerations. In *Physical and chemical constraints on petroleum migration. Vol 1. Notes for AAPG short course.* Ser. 8, pp. B1-B60.

Netzel D. A. and Miknis F. P. (1982) NMR study of US Eastern and Western shale oils produced by pyrolysis and hydropyrolysis. *Fuel* **61**, 1101-1109.

Oh M. S., Taylor R. W., Coburn T. T. and Burnham A. K. (1988) Study of gas evolution during oil shale pyrolysis by TQMS. In *Proc. International Conf. on Oil Shale and Shale Oil* (Edited by Z. Yajie), pp. 295-302. Chemical Industry Press, Beijing.

Péneloux A., Rauzey E., Fréze R. (1982) A consistent correction for Redlich-Kwong-Soave volumes. *Fluid Phase Equilibria* **8**, 7-23.

Peters K. E. (1986) personal communication.

Price L. C., Wenger L. M., Ging T., Blount C. W. (1983) Solubility of crude oil in methane as a function of pressure and temperature. *Org. Geochem.* **4**, 201-221.

Quigley T. M., Mackenzie A. S. and Gray J. R. (1987) Kinetic theory of petroleum generation. In *Migration of Hydrocarbons in Sedimentary Basins* (Edited by B. Doligez), pp. 649-665. Technip, Paris.

Robinson W. E. and Cummins J. J. (1960) Composition of low-temperature thermal extracts from Colorado oil shale. *J. Chem. Eng. Data* **5**, 74-80.

Reynolds J. G., Crawford R. W. and Burnham A. K. (1989) Oil shale pyrolysis by triple quadrupole mass spectrometry: comparisons of gas evolution at 10°C/min heating rate. *Prepr. ACS Div. Fuel Chem.* **34**(4), 1106-1123.

Saxby J. D., Bennett A. J. R., Corcoran J. G., Lambert D. E. and Riley K. W. (1986) Petroleum generation: simulation over six years of hydrocarbon formation from torbanite and brown coal in a subsiding basin. *Org Geochem.* **9**, 69-81.

Soave G. (1972) Equilibrium constants from a modified Redlich-Kwong equation of state. *Chem. Eng. Sci.* **27**, 1197-1203.

Solomon P. R., Hamblen D. G., Carangelo R. M., Serio M. A. and Deshpande G. V. (1988) General model of coal devolatilization. *Energy & Fuels* **2**, 405-422.

Suuberg E. M., Sherman J. and Lilly W. D. (1987) Product evolution during rapid pyrolysis of Green River Formation oil shale. *Fuel* **66**, 1176-1184.

Sweeney J. J., Burnham A. K. and Braun R. L. (1987) A model of hydrocarbon generation from type I kerogen: application to Uinta basin, Utah. *AAPG Bulletin* **71**, 967-985.

Talukdar S., Gallango O., Vallejos C. and Ruggiero A. (1987) Observations on the primary migration of oil in the La Luna source rocks of the Maracaibo basin, Venezuela. In *Migration of Hydrocarbons in Sedimentary Basins* (Edited by B. Doligez), pp. 59-77. Technip, Paris.

Tissot B. P., Deroo G. and Hood A. (1978) Geochemical study of the Uinta basin: formation of petroleum from the Green River formation. *Geochim. Cosmochim. Acta* **42**, 1469-1486.

Tissot B. P., Pelet R. and Ungerer P. (1987) Thermal history of sedimentary basins, maturation indices, and kinetics of oil and gas generation. *AAPG Bulletin* **71**, 1445-1446.

Ungerer P., Bessis F., Chenet P. Y., Durand B., Nogaret E., Chiarelli A., Oudin L., and Perrin J. F. (1984) Geological and geochemical models in oil exploration; principles and practical examples. In *Petroleum geochemistry and Basin Evaluation, AAPG Memoir 35* (Edited by G. Demaison and R. Murris), pp. 53-77. AAPG, Tulsa.

Ungerer P. and Pelet. R. (1987) Extrapolation of kinetics of oil and gas formation form laboratory experiments to sedimentary basins. *Nature* **327**, 52-54.

Wallman P. H., Tamm P. W. and Spars B. G. (1981) Oil shale retorting kinetics. In *Oil Shale, Tar Sands, and Related Materials, ACS Symposium Series* **163** (Edited by H. C. Stauffer), pp. 93-113. American Chemical Society, Washington D. C.

Table 1. Comparison of activation energies (kcal/mol) and distributions (% of E_o) determined by various techniques

Sample	Fluidized bed	Pyromat II E_o	Pyromat II σ	Oil evolution E_o	Oil evolution σ	Hydrous pyrolysis
AP24	51.0a	52.6	1.3	57.5	2.0	66.5[c]
NAKY	50.3[b]	53.0	2.1			
KIMR		54.3	2.7	56.7	3.1	
PHOS		56.3	3.8	62.5	3.5	42.7[d]
WNZN		51.4	2.5	55.7	2.7	
LLNA		52.1	2.6	58.2	2.8	
WDFRD		54.7	3.3			52.2[d]

a. reaction order of 1.18
b. reaction order of 1.44
c. Peters (1986)
d. Lewan (1985)

Table 2. Observed and calculated yields of oil and gas (% of TOC) from pyrolysis of New Albany shale or other marine shales at various heating rates

Conditions	observed		calculated	
	oil	gas	oil	gas
Fluidized bed	45	5	43	4
Fischer assay[a]	33	7	33	4
2°C/min[b]	29	11[c]	31	7
2°C/h[b]	22	13[c]	25	9

a. 12°C/min, no sweep.
b. 50% porosity and no gas sweep
c. by difference

Table 3. Effective rate parameters derived from kinetic analysis of PYROL calculations.

	A (s^{-1})	E (kcal/mol)	σ (% of E)
Green River			
PYROL Input:			
early oil (5%)	1.0×10^{13}	47.0	—
late oil (95%)	1.0×10^{13}	51.0	—
KINETICS Output:			
Slow sweep	2.5×10^{13}	52.1	2.0
Autogenous	8.2×10^{13}	53.7	2.0
Hydrous pyrolysis[a]	1.2×10^{17}	63.7	—
Marine			
PYROL Input	2.4×10^{13}	51.0	3.0
KINETICS Output:			
Slow sweep	4.7×10^{13}	51.7	3.5
Autogenous	1.3×10^{14}	53.1	3.4
Hydrous pyrolysis[a]	5.2×10^{9}	41.8	—

a. first-order kinetic analysis of calculated oil vapor yields from Figures 4 and 5.

Table 4. Calculated products for lacustrine and marine shales as a function of organic content and geological heating rate

Organic carbon (wt%)	Heating rate (°C/My)	Maximum C_{15+} conc. (mg/g TOC)	Oil expelled (mg/g TOC)	API gravity (°API)	Hydrocarbon gas expelled		Hydrocarbon gas retained	
					(mg/g TOC)	(m^3/kg oil expelled)	(mg/g TOC)	(m^3/Mg rock)
Lacustrine								
10	10	126	571	31	87	0.15	34	3.8
	3	112	577	32	98	0.18	27	3.2
	1	105	575	33	108	0.20	21	2.6
3	10	265	345	36	77	0.21	71	2.8
	3	233	402	37	96	0.26	66	2.3
	1	217	422	37	113	0.30	50	1.7
1	10	299	66	47	27	0.46	203	2.3
	3	280	101	47	61	0.72	165	2.0
	1	271	128	47	101	0.97	127	1.5
Marine								
10	10	57	111	37	106	1.0	56	7.0
	3	53	114	37	120	1.1	47	6.4
	1	50	119	37	134	1.2	39	5.4
3	10	72	43	46	60	1.5	112	4.1
	3	67	57	46	91	1.7	83	3.4
	1	65	66	45	115	1.9	64	2.7
1	10	72	5	49	9	2.0	169	2.1
	3	68	8	50	25	3.7	152	2.1
	1	68	11	51	53	6.3	129	1.8

1. Hydrous pyrolysis

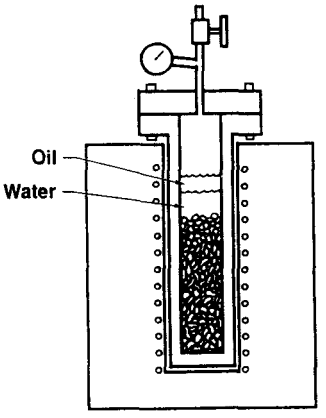

2. Autogenous, self-purging

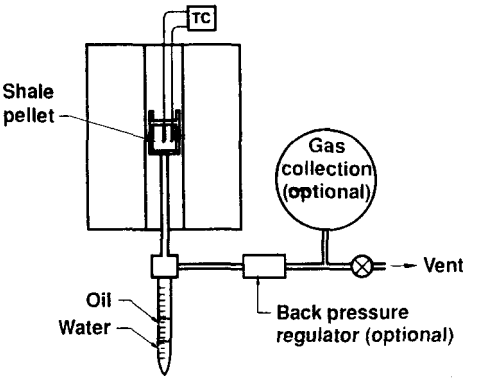

3. Programmed micropyrolysis at multiple heating rates

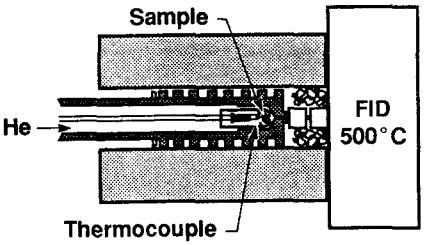

4. Fluidized-bed pyrolysis

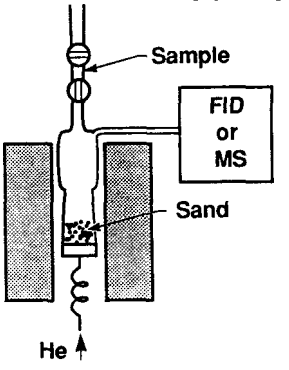

Figure 1. Schematic representation of four types of experiments used in this work to determine oil evolution kinetics. Hydrous pyrolysis results were taken from the literature, the self-purging reactor was operated at 2°C/min and 2°C/h, Rock-Eval and Pyromat instruments were used for nonisothermal micropyrolysis, and the fluidized bed was an LLNL design. In addition, gas evolution kinetics were determined by analyzing the effluent of a small pyrolysis apparatus by tandem mass spectrometry.

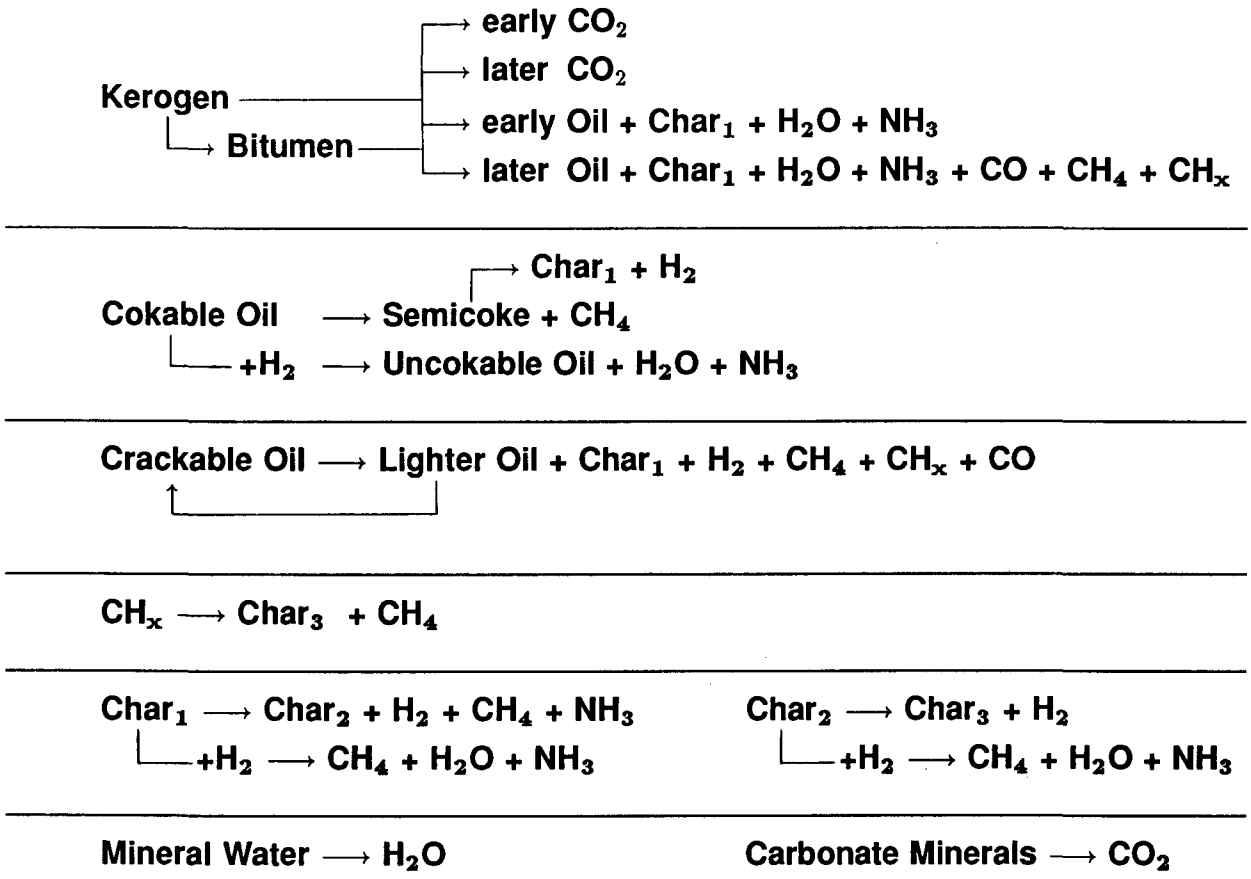

Figure 2. A schematic representation of the chemical reaction framework of PYROL. The complete model consists of time derivatives of 32 vapor species, 32 liquid species, 19 solid species, and 67 other variables, including pore pressure, pore volume, and diagnostics.

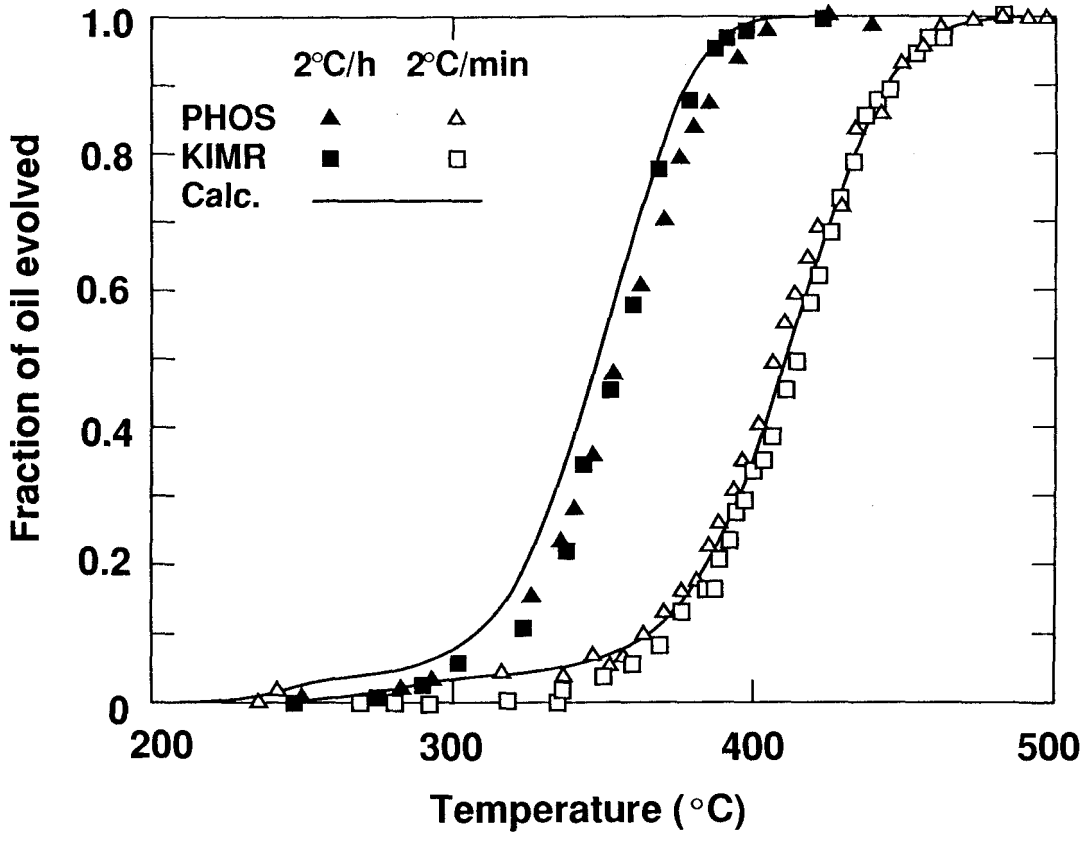

Figure 3. Comparison of the oil evolution rate at 2°C/min and 2°C/h calculated by PYROL with that measured for Kimmeridge (KIMR) and Phosphoria (PHOS) samples.

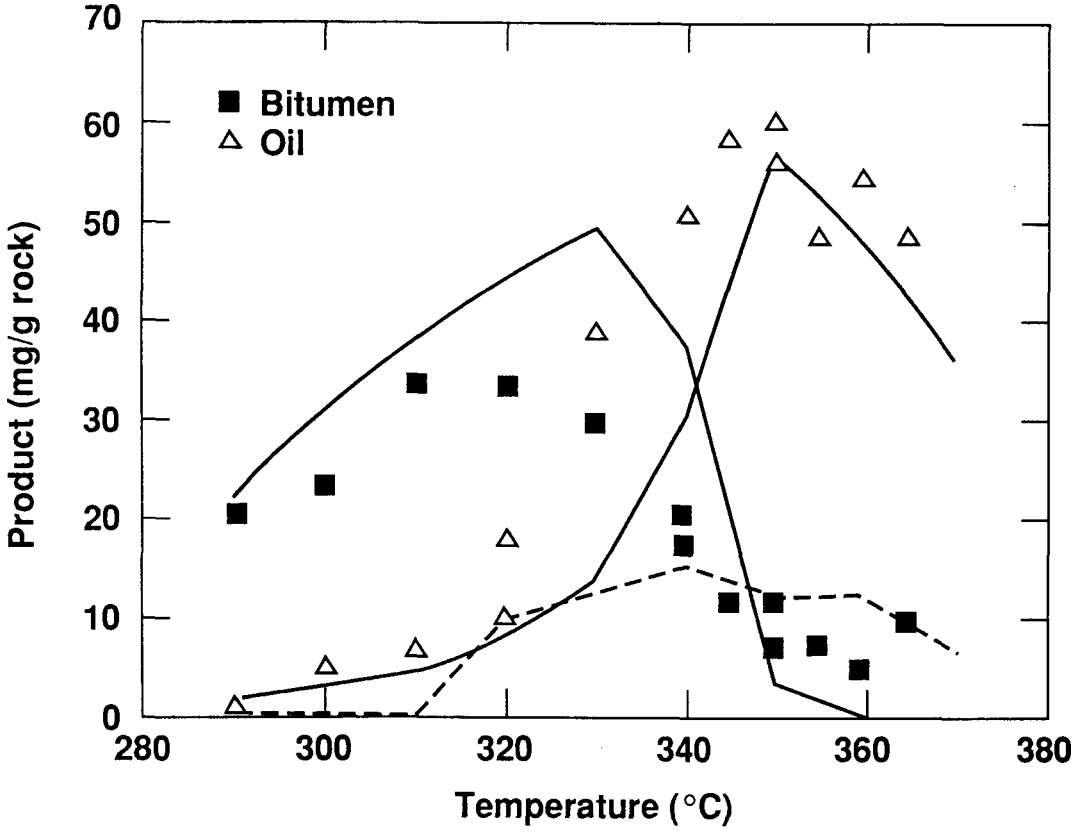

Figure 4. Measured and calculated bitumen and expelled oil yields for Green River shale. The experimental data is from Huizinga *et al.* (1988). The calculated bitumen values are the sum of virtual bitumen, liquid oil and semicoke concentrations from PYROL. The solid calculated curve for expelled oil is the concentration of oil vapor from PYROL, and the dashed curve is the expelled oil calculated from the excess volume generated by pyrolysis.

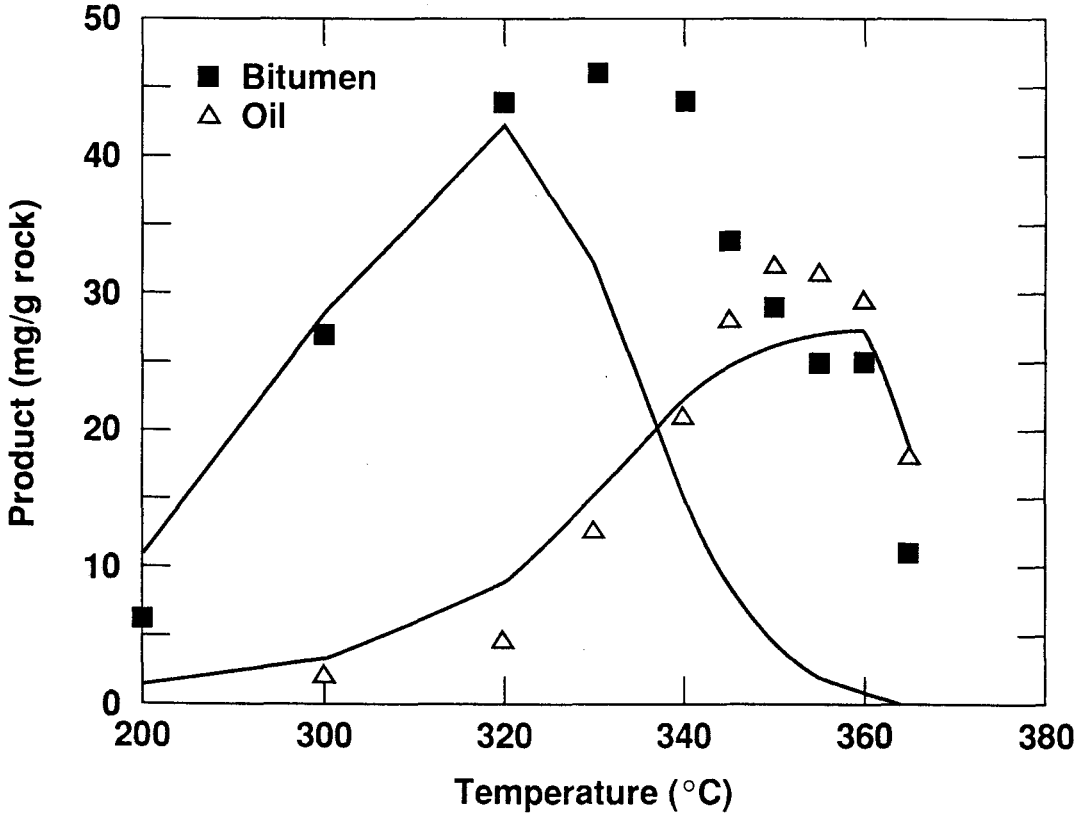

Figure 5. Measured bitumen and expelled oil yields from Woodford shale (Lewan, 1985) compared to PYROL calculations for a generic marine shale with the same organic content. The solid curves represent the same quantities as defined in Figure 4.

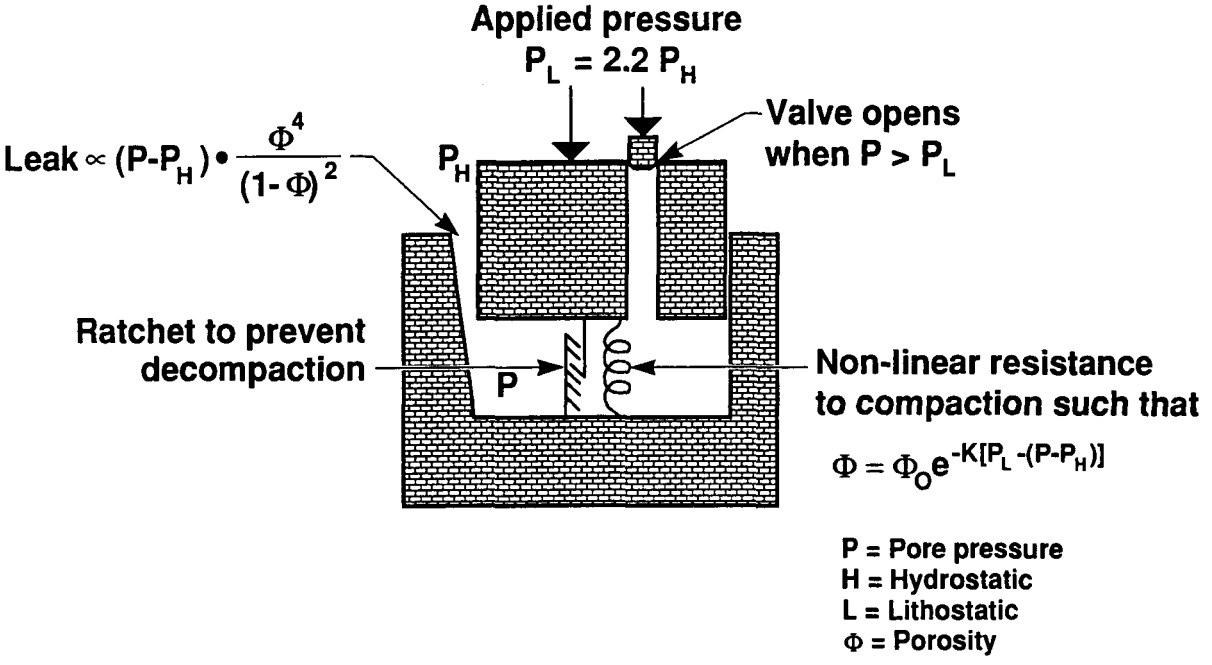

Figure 6. Schematic representation of the compaction model used in PYROL.

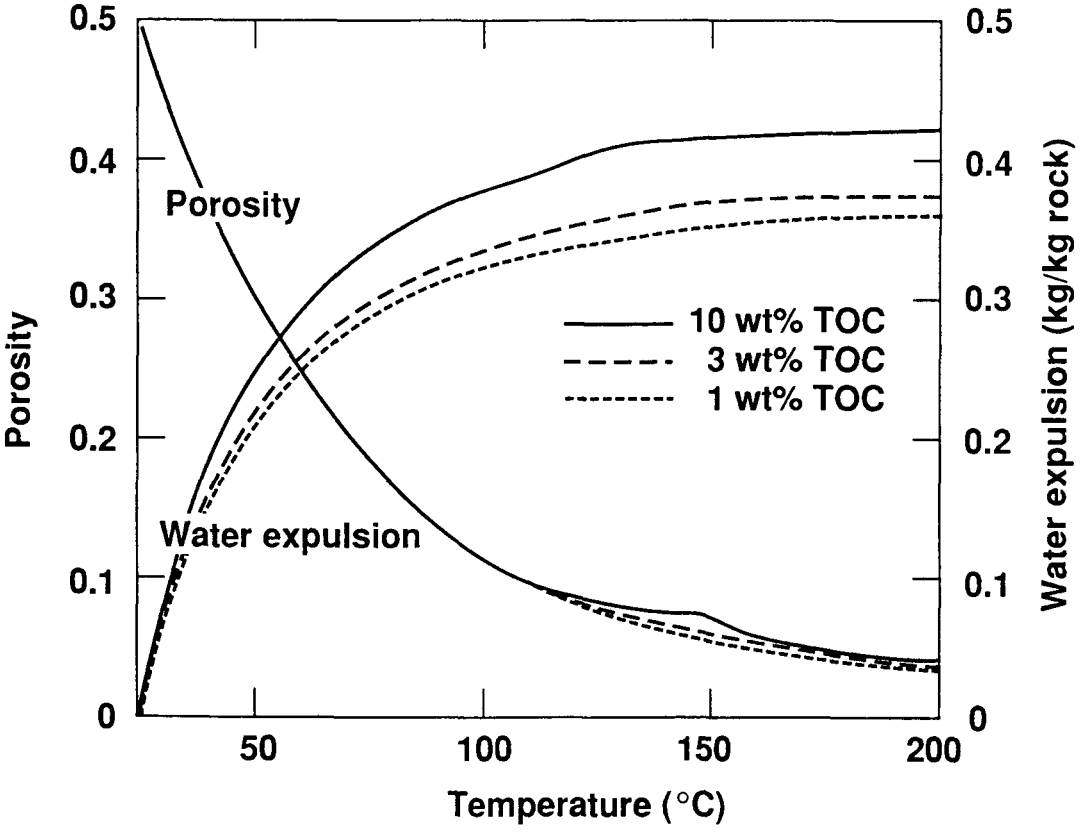

Figure 7. Calculated porosities and cumulative water expelled from a generic marine shales contain 10, 3, and 1 wt% organic carbon heating at 3°C/My assuming a constant geothermal gradient of 25°C/km. The deviation of porosity from and exponential decline with depth is cause by a pressure buildup during oil and gas generation.

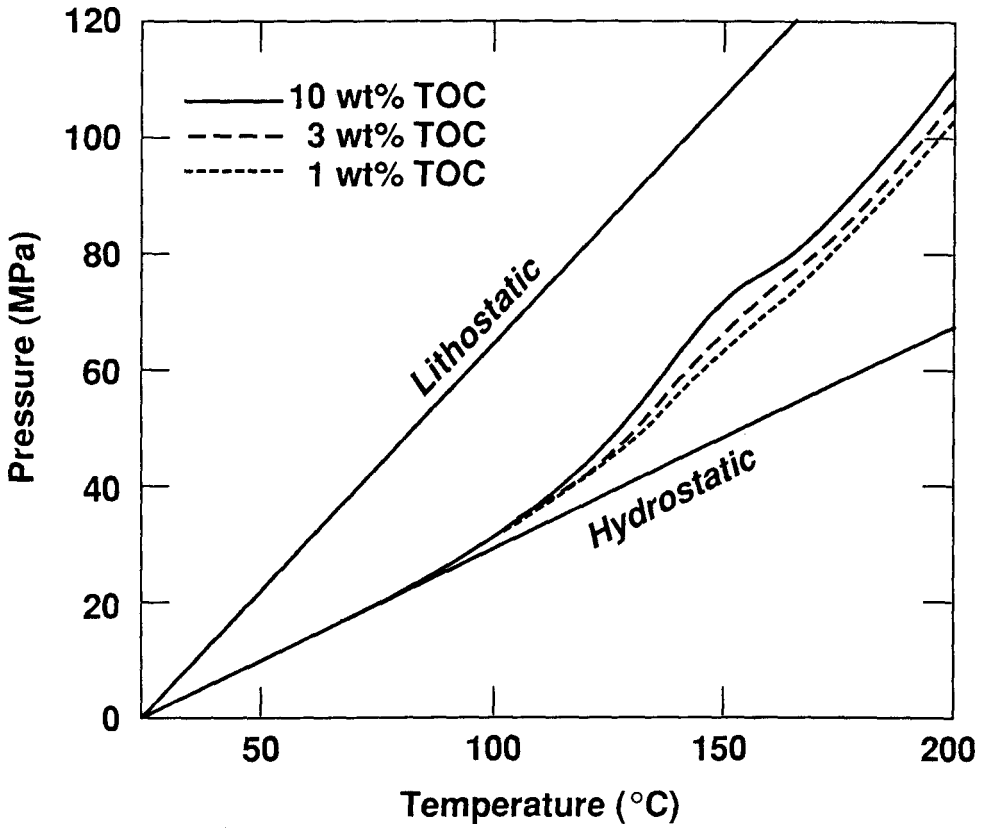

Figure 8. Calculated pore pressures for the same cases shown in Figure 7.

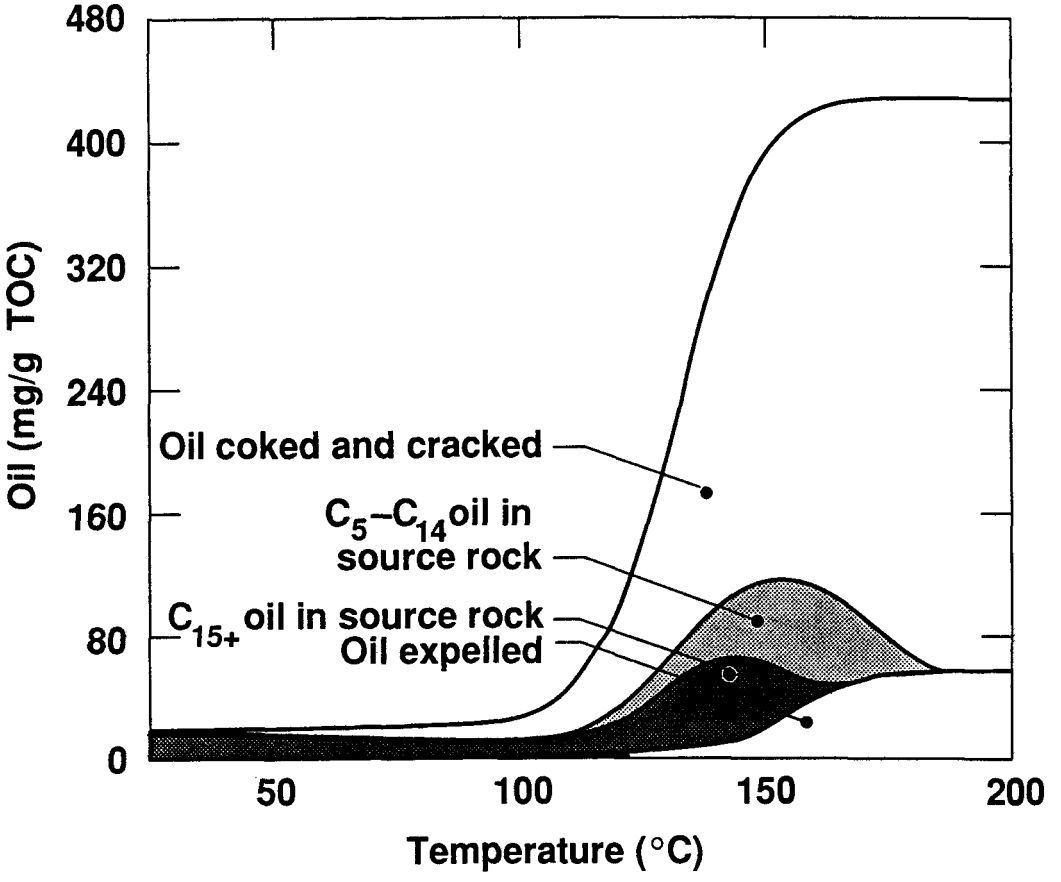

Figure 9. Distribution of generated oil into its various fates, as a function of temperature. The eleven boiling-point oil fractions in the source rock are summed into C_6-C_{14} and C_{15+} fractions. The calculation corresponds to a marine shale containing 3 wt% TOC being heating at 3°C/My in a geothermal gradient of 25°C/km.

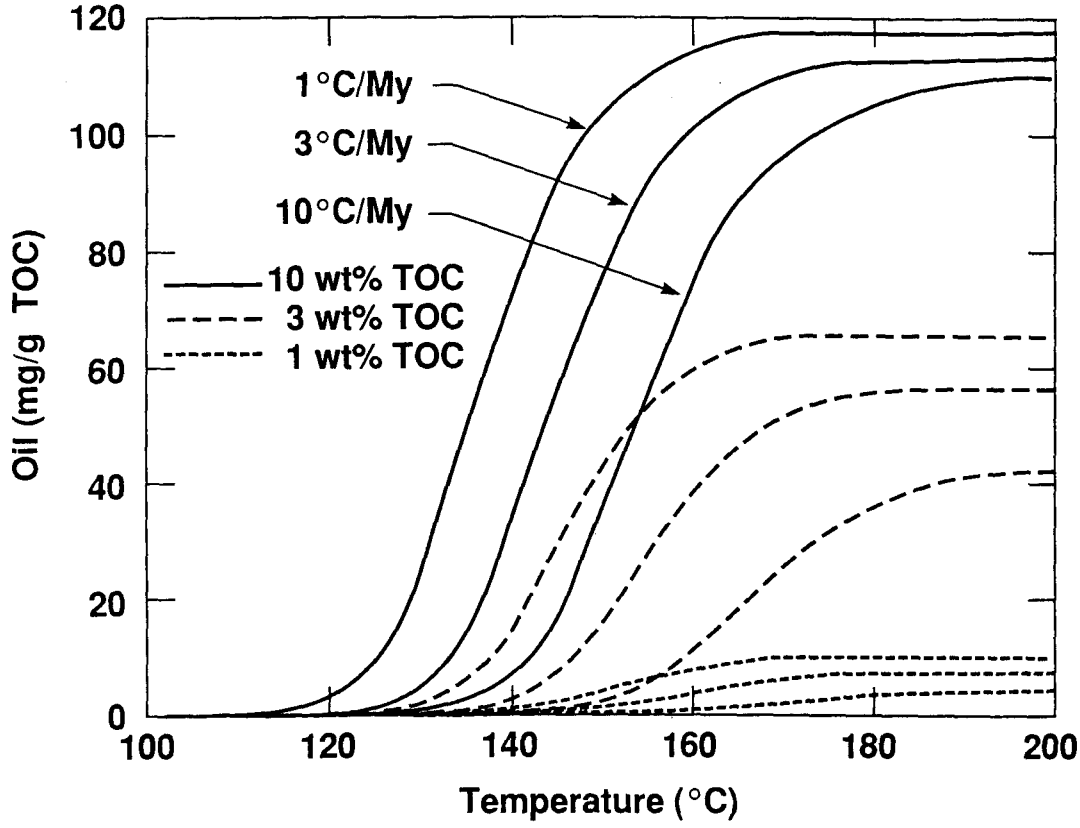

Figure 10. Summary of the oil expulsion curves for generic marine shales.